Materials Research. 2017; 20(3): 826-834
DOI: http://dx.doi.org/10.1590/1980-5373-MR-2016-0751

Effect of an Organo-Modified Montmorillonite on the Barrier Properties of PET Nanocomposites Using a Polyester Ionomer as a Compatibilizing Agent

Suel Eric Vidotti[a]*, Anne Cristine Chinellato[a], Guo-Hua Hu[b], Luiz Antonio Pessan[c]

[a] Centro de Engenharia, Modelagem e Ciências Sociais Aplicadas, Universidade Federal do ABC (CECS/UFABC), Avenida dos Estados, 5001, Bloco A, Torre 1, sala 618, Bairro Santa Terezinha, CEP: 09210-580, Santo André, SP, Brazil
[b] Laboratoire Réactions et Génie des Procédés (CNRS UMR 7274), Ecole Nationale Supérieure des Industries Chimiques (LRGP/ENSIC), Université de Lorraine, 1 rue Grandville, BP 20451, Nancy F-54001, France
[c] Departamento de Engenharia de Materiais, Universidade Federal de São Carlos (DEMa/UFSCar), Via Washington Luiz, km 235, P. O. Box 676, 13565-905 São Carlos, SP, Brazil

Received: October 04, 2016; Revised: March 15, 2017; Accepted: April 21, 2017

Poly(ethylene terephthalate)/organically modified montmorillonite (PET/o-Mt) nanocomposites were prepared via melt intercalation in a twin-screw extruder using a polyester ionomer (PETi) as compatibilizer. The o-Mt content used was 0, 1, 3 or 5 wt% and the compatibilizer/o-Mt mass ratio was 0/1, 1/1 or 3/1. The main objective was to study the effects of the addition of o-Mt and compatibilizer on the barrier properties of PET/o-Mt nanocomposites. The nanocomposites showed a significant reduction in CO_2 permeability of up to 50% when compared to the neat PET, without significant change in the CO_2 solubility revealing the importance of the diffusional path imputed by the organoclay on the overall permeation process. Water vapor permeability was reduced for all nanocomposites, achieving up to 30% reduction for the nanocomposite containing a compatibilizer/o-Mt mass ratio of 1/1. Overall, the nanocomposite containing 5 wt% of organoclay and compatibilizer/o-Mt mass ratio of 1/1 showed the best barrier properties.

Keywords: *PET nanocomposite, Organoclay, Polyester ionomer compatibilizer, Barrier properties, Permeability*

1. Introduction

The use of nano-scale fillers has led to the development of polymer nanocomposites and has provided a potential alternative to conventional polymer composites. Polymer-layered silicate nanocomposites prepared with an organically modified montmorillonite (o-Mt) are of increasing interest for packaging applications. These nanocomposites show improved mechanical and barrier properties compared to the corresponding neat polymer matrix and conventional composites due to the nano-scale reinforcement and the tortuous diffusion path caused by the high aspect ratio of aluminosilicate layers[1-5]. In order to maximize these benefits it is necessary to achieve a high level of organoclay exfoliation, uniform distribution and appropriate orientation of clay platelets[6-9].

Among various processes, the following two are considered as being commercially attractive for preparing layered silicate based polymer nanocomposites: *in situ* polymerization and melt compounding[10,11]. The second one is especially appealing because classical melt compounding equipment and standard processing conditions can be used. Depending on the nature of the components used (layered silicate, organic modifier, polymer matrix and compatibilizer) and preparation process, three main types of composites may be obtained: conventional composite and intercalated or exfoliated nanocomposites[10].

In conventional composites, the polymer is unable to intercalate silicate layers. Thus its properties are not very different from that of traditional microcomposites. Intercalated nanocomposites show a well-ordered multilayered structure (alternating polymer and inorganic layers) in which polymer chains are inserted into the interlayer spaces between individual silicate layers. Exfoliated nanocomposites are achieved when individual silicate layers are completely separated and uniformly distributed in the polymer matrix[10]. Properties of intercalated and exfoliated nanocomposites are usually significantly improved compared to conventional composites or the neat polymer.

However, it is not always possible to reach an intercalated or exfoliated state of dispersion of layered silicate particles by melt compounding[12]. Optimal mixing conditions and adequate surface treatment of silicates should be applied to prepare exfoliated nanocomposites[12-16]. The use of polymers containing polar functional groups and/or ionomers as compatibilizers also promotes the dispersion of silicates and may lead to intercalated and/or exfoliated nanocomposites[17-21].

* e-mail: suel.vidotti@ufabc.edu.br

The gas permeation in a homogeneous polymer matrix is governed by a mechanism of diffusion and solubility. The diffusion coefficient (D) describes the kinetic aspect of the transport whereas the solubility coefficient (S) reflects the penetrant/polymer affinity and the thermodynamic aspect of the transport. In the case of a Fickian transport, the permeability coefficient (P) can be expressed by[22]:

$$P = D.S \quad (1)$$

A similar model has been considered to describe the gas transport properties of composites in which impermeable fillers are dispersed in a polymer matrix. Assuming that the filler does not absorb or conduct the penetrant, the local polymer matrix is not affected by the presence of the filler and the polymer/filler interactions are sufficiently strong enough to avoid void formation at the interfaces, the gas solubility in the composite can be expressed as[23]:

$$S = S_0(1 - \phi) \quad (2)$$

where S_0 is the penetrant solubility coefficient in the pure polymer matrix and ϕ is the volumetric fraction of particles dispersed in the matrix.

In this approximation, the penetrant solubility does not depend on the morphological features of the phases. However, the diffusion process of the penetrant is more complex. The particles act as impenetrable barriers so that the penetrant must follow an elongated (or tortuous) path in order to diffuse through the composite[24]. The diffusion rate of the penetrant is slowed down and can be expressed as:

$$D = D_0/\tau \quad (3)$$

where D_0 is the diffusion coefficient in the neat polymer, D the apparent diffusion coefficient in the nanocomposites and τ the tortuosity.

For semi-crystalline polymers the permeation process is even more complex. Semi-crystalline polymers are discussed as materials consisting of two phases, namely the impermeable crystalline phase and the permeable amorphous matrix. The highly ordered sections hinder the dissolution of small gas molecules and delay diffusion due to the tortuosity caused by the presence of crystalline regions, which are considered impermeable and act similarly to the filler[25].

According to the simple composite theory, this tortuosity factor depends on the volume fraction of particles (ϕ), the particle shape (aspect ratio) and the location and orientation of the particles[23,24]. Combining equations 1 to 3 leads to the following expression for the relative composite permeability:

$$P/P_0 = (1 - \phi)/\tau \quad (4)$$

where P_0 is the permeability coefficient in the neat polymer and P is the permeability coefficient in the nanocomposites.

This work was concerned with the preparation of poly(ethylene terephthalate)/organically modified montmorillonite (PET/o-MT) nanocomposites via melt compounding, using a polyester ionomer as compatibilizer. The main objective was to study the effects of the concentrations of o-MT and compatibilizer on the barrier properties of these nanocomposites.

2. Experimental

2.1. Materials

The PET was obtained from Eastman Chemical (USA). It has an intrinsic viscosity of 0.78-0.84 dL/g and a melting point of 245-255ºC (DSC, ASTM E928). The polyester ionomer compatibilizer (PETi) was obtained from Kemira Chemical (Belgium). It was a sulfonated polyester ionomer with a commercial name of Gerol PS50. According to the technical data sheet of the suppliers, it was soluble in water and had a glass transition temperature of 45 ºC, a molar mass of about 60,000 g/mol and an ionomer content of 13 mol% (dimethyl isophthalate sodium sulfonate ionomer). The organoclay (o-MT) used in this study was Cloisite 20A (d_{001} = 24.2 Å) supplied by Southern Clay Products (USA).

2.2. Preparation of nanocomposites

Nanocomposites were prepared using a co-rotating twin-screw extruder Clextral BC21 (screw diameter = 25 mm and length-to-diameter ratio = 36) with a barrel temperature profile (from the feeding zone to the die) of 20, 255, 250, 240, 250, 235 and 240ºC. The screw speed and feed rate were 100 rpm and 3 kg/h, respectively. The screw profile used was described in a previous paper[21].

Prior to compounding, the PET and PETi were dried for 24 hours at 100 and 60ºC, respectively. The o-MT content was 0, 1, 3 or 5 wt% of the total mass of the composite and the compatibilizer/o-Mt mass ratio was 0/1, 1/1 or 3/1. For each mixture, the components were pre-mixed mechanically at a prescribed ratio and then added to the extruder hopper. The designations of the nanocomposites are as follows: PET-xMyI with x and y indicating the wt% of the Mt and PETi compatibilizer, respectively.

The transmission electronic microscopy (TEM), differential scanning calorimetry (DSC), CO_2 gas sorption, CO_2 permeability and water vapor permeability analyses were performed on thin films (~ 60 µm) prepared by compression molding at 260ºC under 3 ton for 2 min and then quickly cooled in an iced water bath.

2.3. Characterization of nanocomposites

2.3.1. Nanocomposites morphology

For TEM analyses, PET/o-MMT nanocomposites films were microtomed at room temperature in the direction

perpendicular to the press surface using a Leica Reichert Ultracut S50 microtome with a Diatome ultra diamond knife. Samples of 30 to 50 nm thick were then analyzed using a JEOL 100CX Electron Microscope at 100 kV accelerating voltage.

2.3.2. Thermal properties

A Perkin Elmer DSC Pyris 1 was used to analyze the thermal profiles of PET/o-Mt nanocomposites. Samples were heated from 30 to 290ºC at 10ºC/min, kept at 290ºC for 3 min, cooled to 30ºC at 10ºC/min and heated again to 290ºC under N_2 atmosphere. The glass transition temperature (Tg) reported in Table 1 were obtained during the first heating. The melting temperatures (Tm), which correspond to the maximum of the endothermic peak, were obtained for the first and second heating. The degree of crystallinity (X_c) of the films was calculated using equation 5. The value of the melting enthalpy of 100% crystalline PET ($\Delta Hm_{100\%}$) corresponds to 140 J/g[26].

$$X_c = \frac{(\Delta Hm - \Delta Hc_{cold})}{\Delta Hm_{100\%} \cdot \phi_{PET}} \times 100 \quad (5)$$

where ΔHm and ΔHc_{cold} are the melting and cold crystallization enthalpies of the samples in the first heating, respectively; ϕ_{PET} is the mass percentage of the PET in the nanocomposites.

2.3.3. Barrier properties

To measure the amount of CO_2 sorbed at equilibrium (S) in the neat PET and PET/o-Mt nanocomposites, an apparatus and a procedure similar to those described by Koros et al.[27] were used. The sorption isotherms were obtained at 35ºC and the maximum pressure applied was 20 atm.

The CO_2 permeability (P) of PET and PET/o-Mt nanocomposites were measured using a constant volume/variable pressure apparatus[28]. The CO_2 used was of analytical grade. The temperature set at 35ºC and the area of the polymer film was 7.07 cm^2. The upstream pressure was 2, 5 or 10 atm, respectively. The values of permeability (P) were expressed in Barrer [$(cm^3.(STP)cm/(s.cm^2.cmHg) \times 10^{-10}$] and calculated using the following relationship:

$$P = \frac{m_{II}.l.\tilde{V}}{A.(p_1)} \cdot \frac{10^{10}}{5.171493} \quad (6)$$

where m_{II} = permeation rate (moles/s), l = film thickness, $\tilde{V}$ = molar volume, A = permeation area and p_1 = upstream pressure.

The diffusion coefficient (*D*) was calculated from the permeability (*P*) and sorption (*S*) data using the equation 1.

The nanocomposites water vapor permeability was measured by a microgravimetric method based on ASTM E E96/E96M - 10[29]. The parameters were calculated using equations 7 and 8:

$$WVT = \frac{G}{tA} \quad (7)$$

$$P = \frac{WVT}{S} \times e \quad (8)$$

where G = mass variation (g), t = time (h), A= permeation area (m^2), WVT = rate of water vapor transmission (g/m^2h), e = film thickness (m), S = water vapor pressure saturation at the temperature of the experiment (mmHg).

3. Results and Discussion

3.1. Nanocomposites morphology

In this section are presented the results of morphological characterization for samples containing 5 wt% of o-Mt at different compatibilizer concentrations. In general, the micrographs showed a similar trend for the nanocomposites

Table 1. Glass transition temperature (Tg), cold crystallization temperature (Tc_c), crystallization temperature (Tc), melting temperature in the 1st (Tm_1) and 2nd (Tm_2) heating and relative crystallinity for the first (Xc_1) and second heating (Xc_2) for PET and PET/o- Mt nanocomposites.

Sample	Tg[a] (ºC)	Tc_c[a] (ºC)	Tm_1[a] (ºC)	Tc[a] (ºC)	Tm_2[a] (%)	Xc_1[b] (%)	Xc_2[b] (%)
PETi	60	-	-	-	-		
PET	75	125	249	178	248	6.75 ± 0.97	27.74 ± 0.12
PET-1M	74	117	249	197	247	12.71 ± 0.06	32.92 ± 0.16
PET-1M1I	69	115	250	203	250	14.17 ± 0.14	34.18 ± 0.34
PET-1M3I	69	120	250	197	250	10.37 ± 0.21	32.71 ± 0.65
PET-3M	74	115	249	196	249	24.91 ± 0.37	32.98 ± 0.49
PET-3M3I	63	117	248	199	248	19.92 ± 0.60	33.51 ± 1.01
PET-3M9I	62	119	248	195	248	19.26 ± 1.16	35.28 ± 2.12
PET-5M	63	117	249	197	249	25.10 ± 0.63	33.23 ± 0.83
PET-5M5I	64	118	249	199	250	16.86 ± 0.84	32.52 ± 1.63
PET-5M15I	63	120	249	194	249	21.97 ± 2.20	34.64 ± 3.46

[a] Standard deviation ± 1 ºC.

[b] Values obtained according to equation 5.

containing 1 and 3 wt% of o-Mt. For that reason, the TEM micrographs for those nanocomposites were not showed in this section. The main findings are presented to facilitate the correlation with the barrier properties of the materials.

Figure 1 (a) - (f) shows the TEM micrographs of the nanocomposites containing 5 wt% of organoclay. All the nanocomposites presented regions of intercalated o-MMT layers. Moreover, the o-MMT particles were better dispersed in nanocomposites containing PETi. Overall, they were smaller and randomly distributed in the PET matrix[21].

The TEM micrographs indicated the formation of intercalated structure for all nanocomposites. The nanocomposites prepared using the PETi compatibilizer also showed some regions with partial exfoliation.

A complete study of morphology of PET/organoclay nanocomposites using a polyester ionomer as a compatibilizing agent was developed in a previous work[21].

3.2. Thermal properties

Figure 2 shows the DSC thermograms curves for the neat PET and PET/o-Mt nanocomposites containing 5wt% of the o-Mt. The DSC thermograms showed a similar trend for the nanocomposites containing 1 and 3 wt% of o-Mt. Nevertheless, there were small changes in the peak intensity and location. For that reason, the DSC thermograms for the nanocomposites containing 1 and 3 wt% of o-Mt were not showed in this section.

The DSC data for the neat PET and PET/o-Mt nanocomposites are shown in Table 1.

PET/o-Mt nanocomposites showed a decrease in the glass transition temperature (Tg) compared to the neat PET. The systems with the compatibilizer showed a more significant reduction due, probably, to the fact that the Tg of the compatibilizer was lower than that of PET matrix (Table 1). The nanocomposites also showed a decrease in the cold crystallization peaks (Tc_c). Some systems showed slight variations in the melt temperature (Tm_1 and Tm_2). All the nanocomposites showed an increase in the crystallization temperature (Tc) when compared to the neat PET. This behavior is more evident for the nanocomposites with a compatibilizer/organoclay ratio of 1/1 (Table 1, Figure 2 b).

The fact that both the values of Tm and the shape of the melting peak of the PET/o-Mt nanocomposites remained almost unchanged compared to those of neat PET indicates that the organoclay did not affect the perfection and size of the crystals in the polymer matrix[30]. On the other hand, it had a nucleating effect, as observed by the increase of Tc for all nanocomposites. A gradual increase in the relative crystallinity (Xc), compared to neat PET, could also be seen. Xc_1 values were used as the crystallinity degree to calculate nanocomposites and neat PET barrier properties because the films used at permeation and sorption measurements were not annealed prior to test.

3.3. Barrier properties

Figures 3 (a), (b) and (c) show the CO_2 gas permeability of PET nanocomposites. The CO_2 gas permeability of PET/o-Mt nanocomposites was much smaller than that of neat PET.

For samples with 3 wt% of organoclay the permeability decreased gradually with a maximum reduction of 30% at 2 atm while for samples with 5 wt% of organoclay the maximum reduction was about 50%. The organoclay incorporation itself

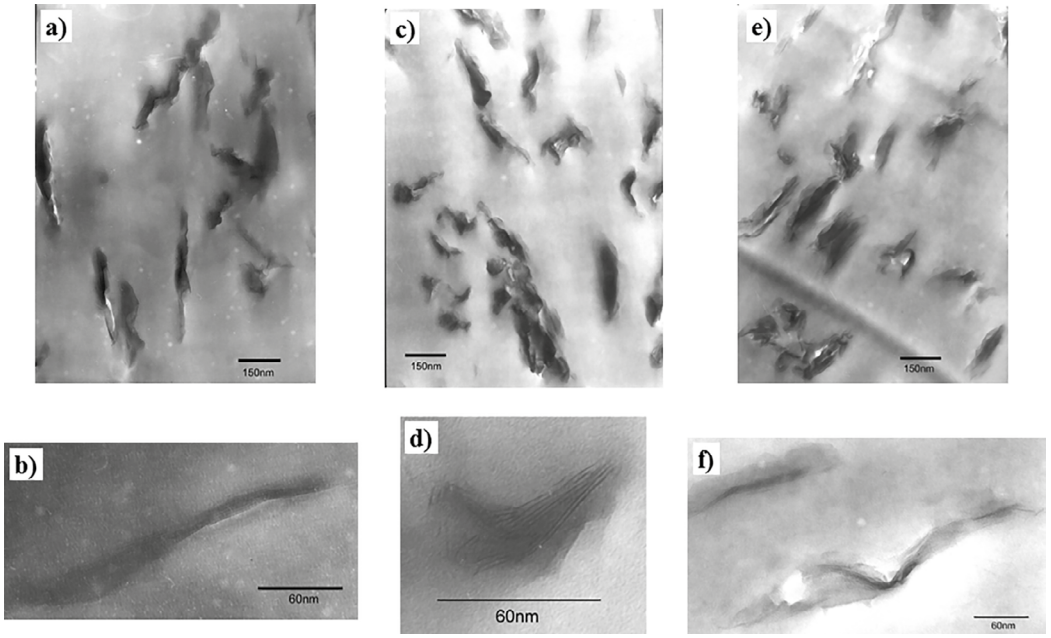

Figure 1. TEM micrographs of PET nanocomposites containing 5 wt% of organoclay. (a-b) PET-5M, (c-d) PET-5M5I, (e-f) PET-5M15I.

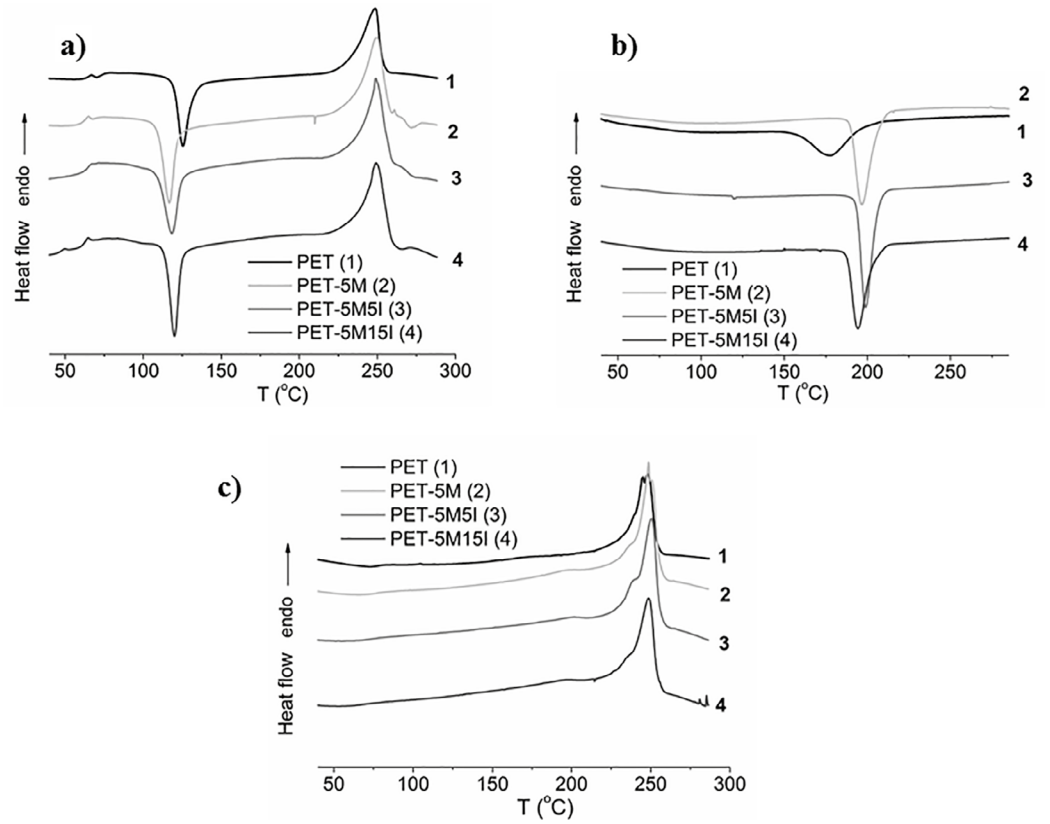

Figure 2. DSC thermograms for the PET and PET/o-Mt nanocomposites containing 5 wt% of organoclay. (a) 1st heating, (b) cooling and (c) 2nd heating.

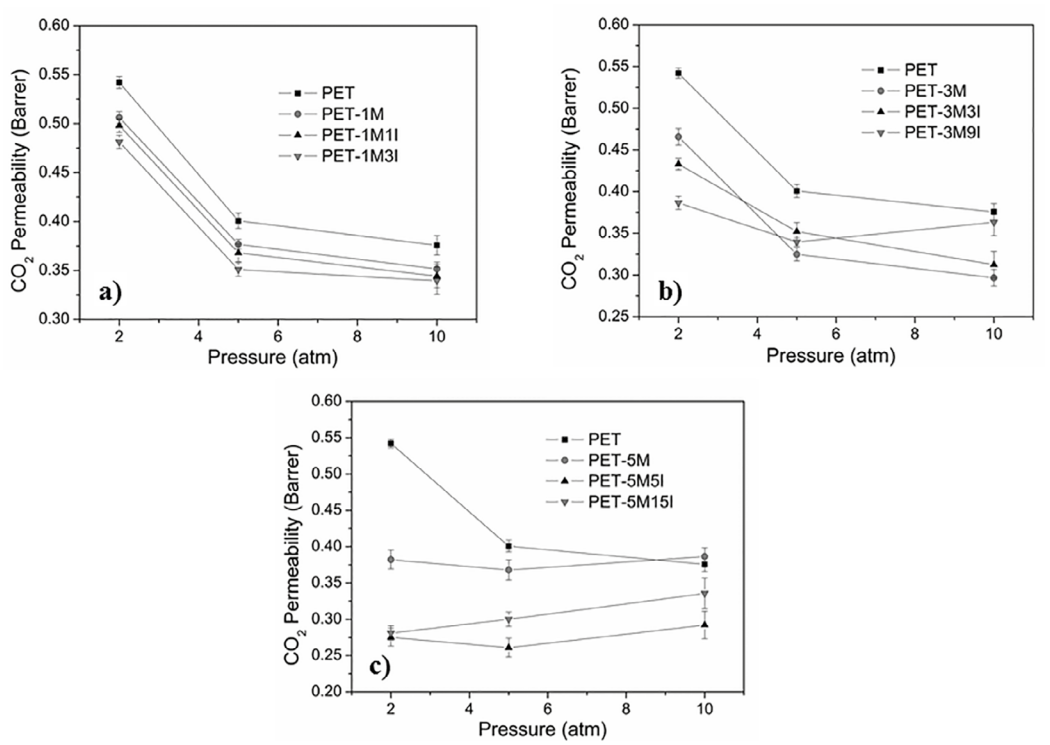

Figure 3. Effect of the compatibilizer concentration on the CO_2 gas permeability of the PET nanocomposites. (a) 1wt%, (b) 3wt% and (c) 5wt% of the organoclay.

led to reduction in permeability. Moreover, this reduction was more observable in samples where the organoclay was better dispersed (intercalation and/or exfoliation), i.e. in the compatibilized samples as revealed by TEM analyses.

The nanocomposites are multiphase systems that present complex transport properties due to the co-existence of phases having different permeability, spatial arrangements and interactions with the polymer matrix. The dispersed phase (silicate) can be considered as being impermeable. The polymeric phase (biphasic system amorphous/crystalline) can be considered as being permeable (amorphous phase) and impermeable (crystalline regions)[28].

For the nanocomposites described in this paper, many factors act simultaneously affecting the CO_2 permeability. The clay, as described previously, can be considered as an impermeable phase, reducing the overall PET permeability. Another effect brought by the clay addition is the increase in crystallinity (nucleating effect), as observed by DSC. The crystallites are also considered as impermeable regions and together with the clay layers help enhance the tortuous diffusion path that the gas molecules have to go through during permeation, according to the Nielsen model[31]. Another factor to be considered is the permeability at the interfaces: polymer/ionomer, polymer/clay, clay/ionomer and polymer/clay/ionomer that are different from that of the pristine PET matrix. Therefore all the above considerations should be taken into account in the analysis of the permeability values obtained.

It is interesting to notice that the nanocomposites containing higher amounts of compatibilizer (PET-3M9I, PET-5M5I and PET-5M15I) showed an increase in permeability at higher CO_2 pressures (Figure 3). This behavior is an indication of polymer matrix plasticization. On the other hand, plasticization was not observed in the neat PET and in the others nanocomposites. In these samples a decrease in permeability with the increase in the CO_2 pressure was observed. This behavior can be associated to the hydrostatic compression of the polymer matrix by the high permeant pressure or due to saturation of the polymer matrix. The plateau observed for the permeability values obtained at higher CO_2 pressure corroborates to these ideas, for the samples where no plasticization phenomenon was observed[28].

As observed, the nanocomposites containing 5 wt% of organoclay exhibited better barrier properties, i.e., more significant reduction in CO_2 permeability, compared with those containing less organoclay. Therefore, the nanocomposites containing 5 wt% of o-Mt were chosen for the CO_2 sorption study. Figure 4 shows CO_2 sorption isotherms at 35ºC.

The sorption isotherms show a similar behavior up to 10 atm., i.e. the penetrant concentration increased linearly with its partial pressure, typical of a Henry's law sorption behavior. At higher CO_2 pressures, there was a change in behavior for neat PET and PET-5M15I. Those samples showed a larger improvement in the equilibrium concentration at higher pressures, indicating that the polymer matrix could have been plasticized by the penetrant (CO_2).

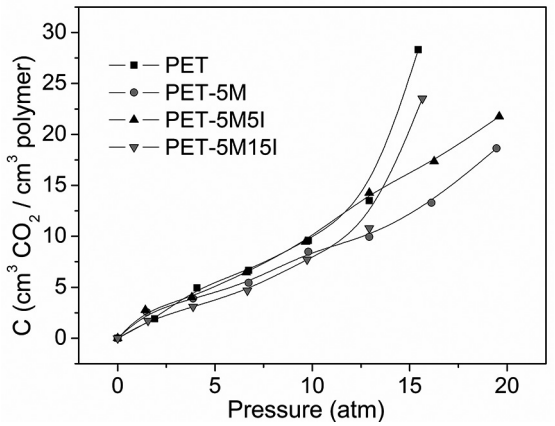

Figure 4. CO_2 sorption isotherms at 35°C for the neat PET and its nanocomposites containing 5 wt% of the organoclay.

This effect can be related to the interaction (solubility) between the gas and the polymer matrix. The CO_2 gas shows high condensability in the polymer matrix and consequently high solubility due to its low critical temperature (31ºC), making plasticization possible[28]. Besides that, at higher gas pressures, the enhanced local concentration of CO_2 could have resulted in an increase of the matrix free volume facilitating the mobility of polymer chains, leading to a further increase in the CO_2 solubility, namely, plasticization. It is important to point out that the samples containing 0 and 5% of compatibilizer did not present any sign of plasticization indicating that the o-Mt dispersion effect to add difficulties to the permeation process prevailed.

The solubility coefficient (S) of the penetrant in the neat PET and its nanocomposites containing 5 wt% of the organoclay at 2, 5, 10 and 15 atm pressures and 35ºC were calculated by equation 9 considering the equilibrium concentration (C_{eq}) of the permeant as a function of the partial pressure (p). The results are presented in Table 2:

$$S = d(C_{eq})/dp \quad \text{(Henry's law)} \qquad (9)$$

Table 2 shows a slight difference in the value of the CO_2 solubility coefficient among the samples in the pressure range studied. Many factors can contribute to the changes in the CO_2 solubility of the PET/o-Mt nanocomposites. For example, the silicate layers could act as impermeable regions, reducing the concentration of absorbed gas. The crystalline regions act the same way. As described previously in DSC analyses, the organoclay incorporation promoted a nucleating effect that reduced the gas sorption of the films. The carbonic chains of the clay modifier instead acted as a permeable region increasing the gas sorption. The compatibilizer (PET ionomer) might have both effects. Its ionic groups result in strong interaction with CO_2 increasing the gas solubility

Table 2. CO_2 solubility coefficient (S) values for the neat PET and PET nanocomposites with 5 wt% of the organoclay at 35ºC.

Sample	S ($cm^3/cm^3.atm$) 2atm	S ($cm^3/cm^3.atm$) 5atm	S ($cm^3/cm^3.atm$) 10atm	S ($cm^3/cm^3.atm$) 15atm
PET	1.07	1.03	1.02	1.83
PET-5M	1.09	0.89	0.83	0.81
PET-5M5I	1.15	1.08	1.06	1.05
PET-5M15I	0.81	0.81	0.80	1.50

(at equilibrium concentration) as observed by Galvani and Pessan[32]. On the other hand, the polar groups contribute to the better dispersion of the organoclay (intercalation and/or partial exfoliation), as revealed by TEM, increasing the impermeable regions in the polymer matrix and so reducing the local concentration of sorbed gas.

The presence of PETi at lower amounts (up to 5%) provides higher sorption values than those of neat PET and those of PET-5M. It is probably due to its high polarity that enables a better interaction between polymeric matrix and permeant. But when used in excess (more than 5%) the effect is the opposite. This behavior can be explained by the Restricted Mobility Model proposed by Eisenberg[33]. According to this model ionomers presents small amounts of ionic aggregates defined as "multiplets" dispersed at the polymeric matrix. Those aggregates are formed due to the electrostatic forces associated to their ionic portions and have restrict mobility around its center.

Increasing the amount of PETi in the composite increases its relative ionic portion. This fact raises the chances to the aggregates to be formed and consequently lowers the amount of ions available to interact with the permeant molecules, leading to lower sorption values that cannot be sustained when high pressures of penetrants are used.

Table 3 shows the apparent diffusion coefficient values (D) calculated from the solubility coefficient (S) and permeability (P) experimental values (equation 1) for the nanocomposites containing 5 wt% of organoclay at different compatibilizer concentration.

Table 3. Values of CO_2 solubility coefficient (S), permeability (P) and diffusion coefficient (D) of the PET/o-Mt nanocomposites at 2 atm.

Sample	S ($cm^3/cm^3.atm$)	P (Barrer)	D (10^{-10} cm^2/s)
PET	1.07	0.54	38.5
PET-5M	1.09	0.38	26.6
PET-5M 5I	1.15	0.27	18.2
PET-5M 15I	0.81	0.28	26.4

According to Table 3, the solubility coefficient (S) of the nanocomposites containing 5wt% of the organoclay was slightly different than that of neat PET. Therefore, the nanocomposites decrease in CO_2 permeability could be attributed to this slight difference and most importantly to a significant decrease in the diffusion path of the CO_2 when the organoclay was incorporated in the PET. This is consistent with the literature[3,10,34]. The presence of the polyester ionomer compatibilizer amplifies this effect due to better o-Mt intercalation and/or exfoliation, as demonstrated by WAXS, TEM and rheological analyses[21]. This effect, in addition to the increase of PET crystallinity (impermeable phase) induced by organoclay, resulted in a decrease in the apparent diffusion coefficient (Table 3) and led to a decrease in permeability (Figure 3).

Table 4 summarizes the values of the CO_2 permeability for the PET/o-Mt nanocomposites at different upstream pressures, calculated from equation 6.

Table 4. CO_2 permeability of PET and PET/o-Mt nanocomposites at different upstream pressures.

Sample	CO_2 Permeability (2 atm)	CO_2 Permeability (5 atm)	CO_2 Permeability (10 atm)
PET	0.542 ± 0.006	0.401 ± 0.008	0.376 ± 0.010
PET-1M	0.506 ± 0.006	0.377 ± 0.005	0.352 ± 0.007
PET-1M1I	0.498 ± 0.007	0.368 ± 0.009	0.344 ± 0.012
PET-1M3I	0.481 ± 0.007	0.351 ± 0.007	0.340 ± 0.0014
PET-3M	0.466 ± 0.010	0.325 ± 0.008	0.297 ± 0.010
PET-3M3I	0.433 ± 0.007	0.352 ± 0.011	0.312 ± 0.016
PET-3M9I	0.387 ± 0.008	0.340 ± 0.005	0.363 ± 0.016
PET-5M	0.382 ± 0.013	0.368 ± 0.014	0.386 ± 0.012
PET-5M5I	0.275 ± 0.012	0.261 ± 0.013	0.292 ± 0.019
PET-5M15I	0.281 ± 0.010	0.300 ± 0.010	0.336 ± 0.021

Overall, the nanocomposites showed significant reduction in CO_2 permeability when compared to the neat PET. This reduction mainly resulted from four factors: the intercalation/exfoliation of the organoclay (physical barrier), the matrix solubility changes as a result of the presence of the compatibilizer (permeant solubility in the matrix), the hydrostatic compression of the polymer matrix by the high pressure of the permeant and polymer matrix crystallinity.

Table 5 shows the water vapor permeability (WVP) of PET/o-Mt nanocomposites. The nanocomposites showed a significant decrease in WVP when compared to neat PET. The highest decrease was about 30% and was obtained with an intermediate compatibilizer/o-Mt mass ratio of 1/1. A further increase in that ratio resulted in an increase in water vapor permeability, due probably to the fact that water was very soluble in the compatibilizer (PETi).

Table 5. Water vapor permeability (WVP) of the PET/o-Mt nanocomposites.

Sample	Water vapor permeability (10^{-10} (g/Pa.s.m))	WVP Reduction (%)
PET	2.77 ± 0.03	-
PET-1M	2.59 ± 0.02	6.5
PET-1M 1I	2.57 ± 0.03	7.2
PET-1M 3I	2.54 ± 0.04	8.3
PET-3M	2.38 ± 0.03	14.1
PET-3M 3I	2.35 ± 0.04	15.2
PET-3M 9I	2.44 ± 0.05	11.9
PET-5M	2.01 ± 0.02	27.4
PET-5M 5I	1.98 ± 0.06	28.5
PET-5M 15I	2.32 ± 0.05	16.2

The factors mentioned above that influence the CO_2 permeability of the nanocomposites also influence their water vapor permeability. Moreover, for the water vapor permeability there is a trade-off between the apparent diffusion coefficient (D) and solubility (S). On the one hand, the presence of the PET ionomer compatibilizer decreases D due to better organoclay dispersion (intercalation and/or partial exfoliation). On the other hand, S is increased because water is very soluble in the compatibilizer. Both effects dictate the overall permeability of water vapor in the PET/o-Mt nanocomposites.

4. Conclusions

This work was aimed at studying the influence of using a modified montmorillonite on the barrier properties of PET nanocomposites using a polyester ionomer (PETi) as compatibilizer. Overall, for the nanocomposites studied in this paper, the incorporation of the organoclay increases the diffusional path of penetrant (CO_2, water vapor) leading to permeability reduction.

The compatibilizer (PETi) improves the organoclay dispersion and so reduces the CO_2 permeability. On the other hand, at higher concentrations, the PETi increases the solubility of the penetrant in the polymer matrix due to its polar groups and consequently increases the permeability compared to the results obtained for lower pressures of CO_2. At low CO_2 pressures the organoclay dispersion is the major factor that affects permeability. Besides that, at higher pressures, the penetrant's solubility takes an important role in permeability. The incorporation of the compatibilizer to the PET/o-Mt system led to a decrease of up to 49% in CO_2 permeability (for the sample PET5M5I).

The water vapor permeability in the nanocomposites was also reduced compared to that of the neat PET. The highest diminution was about 28% and was obtained for the samples PET5M and PET5M5I. A further increase in the compatibilizer/o-Mt ratio resulted in an increase in water vapor permeability, due probably to the solubility of water in the compatibilizer. The PET/o-Mt nanocomposite containing 5 wt% organoclay and 5 wt% compatibilizer showed the most significant reduction both in CO_2 and water vapor permeability.

The results indicate that the permeation mechanism is, as well known, highly influenced by the matrix/penetrant pair but also that the penetrant pressure can invert the importance of isolated contribution of sorption/diffusion process even when the system studied is submitted to the incorporation of a physical barrier for the penetrants, as is the case of the o-Mt.

5. Acknowledgements

The authors would like to thank CAPES for the financial support, Mr. J-M Hiver for WAXS measurements, Dr. N.M. Larocca for TEM analyses, PPG-CEM/UFSCar, DEMa/UFSCar and LRGP/ENSIC for research facilities.

6. References

1. Zanetti M, Lomakin S, Camino G. Polymer layered silicate nanocomposites. *Macromolecular Materials and Engineering*. 2000;279(1):1-9.

2. Ray SS, Okamoto M. Polymer/layered silicate nanocomposites: a review from preparation to processing. *Progress in Polymer Science*. 2003;28(11):1539-1641.

3. Picard E, Espuche E, Fulchiron R. Effect of an organo-modified montmorillonite on PLA crystallization and gas barrier properties. *Applied Clay Science*. 2011;53(1):58-65.

4. Ghanbari A, Heuzey MC, Carreau PJ, Ton-That MT. Morphology and properties of polymer/organoclay nanocomposites based on poly(ethylene terephthalate) and sulfopolyester blends. *Polymer International*. 2013;62(3):439-448.

5. Seethamraju S, Ramamurthy PC, Madras G. Performance of an ionomer blend-nanocomposite as an effective gas barrier material for organic devices. *RSC Advances*. 2014;4(22):11176-11187.

6. Shah RK, Krishnaswamy RK, Takahashi S, Paul DR. Blown films of nanocomposites prepared from low density polyethylene and a sodium ionomer of poly(ethylene-co-methacrylic acid). *Polymer*. 2006;47(17):6187-6201.

7. Hu GH, Hoppe S, Feng LF, Fonteix C. Nano-scale phenomena and applications in polymer processing. *Chemical Engineering Science*. 2007;62(13):3528-3537.

8. Vermogen A, Masenelli-Varlot K, Séguéla R, Duchet-Rumeau J, Boucard S, Prele P. Evaluation of the Structure and Dispersion in Polymer-Layered Silicate Nanocomposites. *Macromolecules*. 2005;38(23):9661-9669.

9. Issaadi K, Habi A, Grohens Y, Pillin I. Effect of the montmorillonite intercalant and anhydride maleic grafting on polylactic acid structure and properties. *Applied Clay Science*. 2015;107:62-69.

10. Alexandre M, Dubois P. Polymer layered-silicate nanocomposites: preparation, properties and uses of a new class of materials. *Materials Science and Engineering: R: Reports*. 2000;28(1-2):1-63.

11. Cho JW, Paul DR. Nylon 6 nanocomposites by melt compounding. *Polymer*. 2001;42(3):1083-1094.

12. Vaia RA, Jandt KD, Kramer EJ, Giannelis EP. Kinetics of Polymer Melt Intercalation. *Macromolecules*. 1995;28(24):8080-8085.

13. Dennis HR, Hunter DL, Chang D, Kim S, White JL, Cho JW, et al. Effect of melt processing conditions on the extent of exfoliation in organoclay-based nanocomposites. *Polymer*. 2001;42(23):9513-9522.

14. Fornes TD, Yoon PJ, Hunter DL, Keskkula H, Paul DR. Effect of organoclay structure on nylon 6 nanocomposite morphology and properties. *Polymer*. 2002;43(22):5915-5933.

15. Frounchi M, Dourbash A. Oxygen Barrier Properties of Poly(ethylene terephthalate) Nanocomposite Films. *Macromolecular Materials and Engineering*. 2009;294(1):68-74.

16. Tsai TY, Lin MJ, Chuang YC, Chou PC. Effects of modified Clay on the morphology and thermal stability of PMMA/clay nanocomposites. *Materials Chemistry and Physics*. 2013;138(1):230-237.

17. Barber GD, Calhoun BH, Moore RB. Poly(ethylene terephthalate) ionomer based clay nanocomposites produced via melt extrusion. *Polymer*. 2005;46(17):6706-6714.

18. Ammala A, Bell C, Dean K. Poly(ethylene terephthalate) clay nanocomposites: Improved dispersion based on an aqueous ionomer. *Composites Science and Technology*. 2008;68(6):1328-1337.

19. Chinellato AC, Vidotti SE, Hu GH, Pessan LA. An acrylic acid modified polypropylene as a compatibilizing agent for the intercalation/exfoliation of an organically modified montmorillonite in polypropylene. *Journal of Polymer Science Part B: Polymer Physics*. 2008;46(17):1811-1819.

20. Dini M, Mousavand T, Carreau PJ, Kamal MR, Ton-That MT. Microstructure and properties of poly(ethylene terephthalate)/organoclay nanocomposites prepared by water-assisted extrusion: Effect of organoclay concentration. *Polymer Engineering & Science*. 2014;54(8):1879-1892.

21. Vidotti SE, Chinellato AC, Hu GH, Pessan LA. Preparation of poly(ethylene terephthalate)/organoclay nanocomposites using a polyester ionomer as a compatibilizer. *Journal of Polymer Science Part B: Polymer Physics*. 2007;45(22):3084-3091.

22. Comyn J. *Polymer Permeability*. Dordrecht: Springer Netherlands; 1985.

23. Picard E, Vermogen A, Gérard JF, Espuche E. Barrier properties of nylon 6-montmorillonite nanocomposite membranes prepared by melt blending: Influence of the clay content and dispersion state: Consequences on modelling. *Journal of Membrane Science*. 2007;292(1-2):133-144.

24. Choudalakis G, Gotsis AD. Permeability of polymer/clay nanocomposites: A review. *European Polymer Journal*. 2009;45(4):967-984.

25. Koros WJ, Hellums MW. Transport properties. In: *Encyclopedia of polymer science and engineering*. New York: John Wiley & Sons; 1989. p. 724-802.

26. Wunderlich B. *Thermal Analysis of Polymeric Materials*. Berlin/Heidelberg: Springer-Verlag; 2005.

27. Koros WJ, Paul DR, Rocha AA. Carbon dioxide sorption and transport in polycarbonate. *Journal of Polymer Science Part B: Polymer Physics*. 1976;14(4):687-702.

28. Chinellato AC, Vidotti SE, Hu GH, Pessan LA. Compatibilizing effect of acrylic acid modified polypropylene on the morphology and permeability properties of polypropylene/organoclay nanocomposites. *Composites Science and Technology*. 2010;70(3):458-465.

29. ASTM International. *ASTM E96/E96M - 10 Standard test Methods for Water Vapor Transmission of Materials*; West Conshohocken: ASTM International; 2010. p. 1-12.

30. Vidotti SE, Chinellato AC, Boesel LF, Pessan LA. Poly(Ethylene Terephthalate)-Organoclay Nanocomposites: Morphological, Thermal and Barrier Properties. *Journal of Metastable and Nanocrystalline Materials*. 2004;22:57-64.

31. Nielsen LE. Models for the Permeability of Filled Polymer Systems. *Journal of Macromolecular Science: Part A - Chemistry*. 1967;1(5):929-942.

32. Galvani F, Pessan LA. Effects of Addition of a Polyester Ionomers in the Structure and Crystallinity of Poly(ethylene terephthalate) (PET). In: *7º Congresso Brasileiro de Polímeros*; 2003 Nov 9-13; Belo Horizonte, MG, Brazil.

33. Eisenberg A. Ionic forces in polymers. In: *Fortschritte der Hochpolymeren-Forschung*. Berlin/Heidelberg: Springer-Verlag; 1967. p.59-112.

34. Slavutsky AM, Bertuzzi MA. Thermodynamic study of water sorption and water barrier properties of nanocomposite films based on brea gum. *Applied Clay Science*. 2015;108:144-148.